Journal of Solid State Chemistry 184 (2011) 1227–1235

Contents lists available at ScienceDirect

Journal of Solid State Chemistry

journal homepage: www.elsevier.com/locate/jssc

Controlled synthesis of monodispersed $AgGaS_2$ 3D nanoflowers and the shape evolution from nanoflowers to colloids

Yanping Yuan [a], Jiantao Zai [a], Yuezeng Su [b], Xuefeng Qian [a,*]

[a] School of Chemistry and Chemical Engineering, State Key Laboratory of Metal Matrix Composites, Shanghai Jiao Tong University, Shanghai 200240, PR China
[b] School of Aeronautics and Astronautics, Shanghai Jiao Tong University, Shanghai 200240, PR China

ARTICLE INFO

Article history:
Received 10 March 2011
Accepted 10 March 2011
Available online 6 April 2011

Keywords:
Mixed solvent
Ternary chalcogenides
$AgGaS_2$
Nanoflowers
Colloids

ABSTRACT

Monodispersed $AgGaS_2$ three-dimensional (3D) nanoflowers have been successfully synthesized in a "soft-chemical" system with the mixture of 1-octyl alcohol and cyclohexane as reaction medium and oleylamine as surfactant. The crystal phase, morphology and chemical composition of the as-prepared products were characterized by X-ray diffraction (XRD), transmission electron microscopy (TEM), and high-resolution TEM (HTEM), respectively. Results reveal that the as-synthesized $AgGaS_2$ nanoflowers are in tetragonal structure with 3D flower-like shape. Controlled experiments demonstrated that the shape transformation of $AgGaS_2$ nanocrystals from 3D nanoflowers (50 nm) to nanoparticles (10–20 nm) could be readily realized by tuning the reaction parameters, e.g., the ratio of octanol to cyclohexane, the length of carbon chain of fatty alcohol, the concentration of oleylamine, etc. The UV–vis and PL spectra of the obtained $AgGaS_2$ nanoflowers and colloids were researched. In addition, the photoelectron energy conversion (SPV) of $AgGaS_2$ nanoflowers was further researched by the surface photovoltage spectra.

1. Introduction

It is generally acceptable that the precise control of the chemical composition, crystal structure, size, shape and surface chemistry of nanomaterials allows one to observe their unique properties and to tune their chemical and physical properties as desired [1–5]. Thus, controlled synthesis of nanomaterials had been focused not only on their fundamental shape- and size-dependent properties and important technological applications, but also on their self-assembly for device applications. Up to now, though great progresses have been achieved in the controlled synthesis of monodispersed binary chalcogenide or other functional compound colloids through the organic solution phase pyrolysis approach and its alternatives in diverse precursors, surfactants or solvent system [6,7], the researches on ternary chalcogenide colloids have been largely lagged far behind because of the lack of suitable synthetic methods.

As a fascinating group of inorganic-functional materials, ternary chalcogenides of *I–III–VI* (*I*=Cu, Ag; *III*=Ga, In; and *VI*=S, Se, Te) usually exhibit unique chemical and physical properties and have important technological applications in the areas of photovoltaic devices, light emitting diodes, linear and nonlinear optical instruments, etc. [2,8–11]. Therefore, many efforts have been focused on them in the past years, and *I–III–VI* nanomaterials with different compositions and/or various shapes have been fabricated by different synthetic routes. For instance, $CuInS_2$ and $AgInS_2$ nanocrystals with various shapes (including particles, rods, and worms) have been prepared through wet-chemistry progress assisted by various surfactants or ligands [12–15]. Some ternary chalcogenide colloids were prepared through solvothermal method with the presence of octadecylamine or through the organic solution phase pyrolysis approach, such as $AgInS_2$, $CuInS_2$, $ZnIn_2S_4$, and $AgInSe_2$ [13–17]. Recently, monodispersed pyramidal $CuInS_2$ and rectangular $AgInS_2$ colloids were also successfully synthesized in our group [18]. As the follow-up research, we further extended our research to synthesize other ternary compounds, such as the monodispersed $AgGaS_2$ nanocrystals.

Silver thiogallate ($AgGaS_2$) was chosen as the object because it was one of the important members in the large family of *I–III–VI* (*I*=Cu, Ag; *III*=Ga, In; and *VI*=S, Se, Te) compounds with the band gap of 2.7 eV. It usually exhibits a variety of interesting properties (i.e., optical nonlinearity, birefringence, optical activity, etc.) [19–21], and has wide applications in nonlinear optical devices, e.g. second harmonic generators, optical parametric oscillators, upconverters, etc. [21]. Traditionally, $AgGaS_2$ was prepared via high-temperature solid state reaction [22], vacuum evaporation [23], and hydrothermal or solvothermal reaction route [24,25]. However, the obtained products are often in irregular shape or

* Corresponding author. Fax: +86 21 54741297.
E-mail address: xfqian@sjtu.edu.cn (X. Qian).

0022-4596/$ - see front matter © 2011 Elsevier Inc. All rights reserved.
doi:10.1016/j.jssc.2011.03.022

conglomeration with large size-distribution, which might affect the future application. High quality $AgGaS_2$ nanocrystals with desired shape and size have few been reported. In general, the synthesis of *I–III–VI* ternary component nanocrystals was usually limited by the reactivity difference of precursors and the phase separation of alloy constituents because the separated nuclei might be generated and grown into two binary compounds if the reaction activities of two metal precursors differ much from each other [2,13,26]. Therefore, how to choose the appropriate reaction parameters (e.g. solvents, surfactants, temperature, time, etc.) for controlling the composition, size, shape and structure of $AgGaS_2$ nanocrystals, especially for the phase formation, still remains a great challenge.

In present work, a mixed solvent reaction system (noncoordinating cyclohexane and 1-octyl alcohol/other alcohols) with oleylamine (OA) as surfactant was elaborately designed to prepare ternary chalcogenide $AgGaS_2$, and monodispersed nanomaterials with controlled shape and size were successfully obtained with simple inorganic salts as precursors. Further studies revealed that the morphology of the obtained $AgGaS_2$ could undergo a transformation from 3D nanoflowers to colloids nanoparticles by simply adjusting the reaction parameters, e.g., the ratio of cyclohexane and 1-octyl alcohol, the carbon chain length of alcohol, and the molar ratio of OA. To the best our knowledge, such kind of $AgGaS_2$ 3D nanoflowers synthesized in a mixed solution has not yet been reported. This simple reaction system also provides a new approach to synthesize ternary nanomaterials and understand the reaction mechanism along with the growth kinetics of nanocrystals

2. Materials and methods

2.1. Materials

Sliver acetate (AgAc), carbon disulfide, 1-propyl alcohol (PPA), 1-pentyl alcohol (PTA), 1-octyl alcohol (OTA), 1-dodecyl alcohol (DDA), oleyl alcohol (OEA), cyclohexane (CHA), and gallium (Ga) are analytical reagents and purchased from Shanghai Chemical Reagent Corp.; Oleylamine (OA) (90% mass fraction) is purchased from J & K CHEMICAL LTD. All reagents are used as received without further purification.

2.2. Synthesis

2.2.1. $GaCl_3$ precursor synthesis

$GaCl_3$ was prepared by dissolving Ga in hydrochloric acid solution to form $GaCl_3$ aqueous solution (48 h and 120 °C), and removing H_2O and HCl by rotary evaporation. Then, the final product was reserved in the dehumidifier.

2.2.2. $AgGaS_2$ synthesis

$AgGaS_2$ nanomaterials were synthesized in a mixed solvent by a solvothermal process. In a typical experiment, 0.3 mmol AgAc (AR) and 3 mmol oleylamine (OA) were added to the mixed solvent (40 ml) of 1-octyl alcohol (OTA) and cyclohexane (vol: 1:1) at room temperature, and then homogenous solution was obtained by vigorous magnetic stirring for 1 h. After that, the mixed solution was transferred into a Teflon-lined stainless steel autoclave with a capacity of 40 ml, and then 0.3 mmol $GaCl_3$ and 0.5 ml carbon disulfide were added under magnetic stirred. After the autoclave was sealed and maintained in a preheated oven at 180 °C for 12 h, it was moved and cooled to ca. 60 °C naturally. Precipitates appeared when adding methanol into the colloidal solution. Final products were collected followed by repeated washing with absolute ethanol and drying in vacuum oven at 60 °C. The as-prepared nanomaterials could be easily re-dispersed in organic solvents, such as chloroform, toluene, etc. Detailed experiment parameters and the corresponding results of $AgGaS_2$ are summarized in Table 1.

2.3. Characterization

The phase of the as-prepared products was characterized by a Rigaku D/Max-2200PC diffractometer equipped with a rotating anode and a Cu $K\alpha$ radiation sourse (λ=0.15418 nm), 2θ ranging from 20° to 70° at a scanning rate of 6°/min. The morphology, crystal lattice and chemical composition of the obtained samples were characterized by transmission electron microscopy (Philips Tecnai-12, with an accelerating voltage of 120 kV), high-resolution transmission electron microscopy (JEOL JEM-2100 F, with an accelerating voltage of 200 kV) and energy-dispersive X-ray analysis (EDS) spectroscopy (JEOL JSM—6460 with an accelerating voltage of 5 kV). Solid scattered reflection spectra were

Table 1
Detailed experimental parameters and the corresponding results of $AgGaS_2$.

Sample	Alcohol V (ml)	CHA (ml)	OA/Ag^+	T (°C)	t (h)	Morphologies
1	OTA, 16	16	10	180	12	Monodispersed nanoflowers
2	OTA, 3	30	10	180	12	Nanoflowers
3	OTA, 5.5	27.5	10	180	12	Nanoflowers
4	OTA, 27.5	5.5	10	180	12	Nearly colloids
5	OTA, 30	3	10	180	12	Colloids
6	PPA, 16	16	10	180	12	Nanoflowers
7	PTA, 16	16	10	180	12	Nanoflowers
8	DDA, 16	16	10	180	12	Colloids
9	OEA, 16	16	10	180	12	Colloids
10	OTA, 16	16	3	180	12	Spherical particles
11	OTA, 16	16	6	180	12	Spherical particles
12	OTA, 16	16	12	180	12	Irregularly particles
13	OTA, 16	16	15	180	12	Colloids
14	OTA, 16	16	10	180	3	Nanoflowers
15	OTA, 16	16	10	180	6	Nanoflowers
16	OTA, 16	16	10	180	24	Monodispersed nanoflowers
17	OTA, 16	16	10	180	48	Larger nanoflowers
18	OTA, 16	16	10	180	72	Nearly colloids
19	OTA, 16	16	10	120	12	Aggregated particles
20	OTA, 16	16	10	140	12	Nanoflowers
21	OTA, 16	16	10	160	12	Nanoflowers
22	OTA, 16	16	10	200	12	Nanoflowers

recorded on UV–vis spectrometer (UV-2450 SHIMADAZU). PL spectra were measured on Fluorolog-3-P (Jobin Yvon), and a He–Cd laser with wavelength of 405 nm was used as excitation source for steady-state PL measurement at room temperature. The instrument for measuring the surface photovoltage spectroscopy (SPS) of samples was made by ourselves. Monochromatic light was obtained by passing light from 500 W xenon lamp (CHF XQ500, Global xenon lamp power made in China) through a double-prism monochromator (Hilger and Watts, D 300 made in England). The slit width of entrance and exit is 1 mm. A lock-in amplifier (SR830- DSP, made in USA), synchronized with a light chopper (SR540, made in USA), was employed to amplify the photovoltage signal. The range of modulating frequency is from 20 to 70 Hz, and the spectral resolution is 1 nm.

3. Results and discussion

3.1. Morphological, crystal phase and compositional characterization of $AgGaS_2$ nanomaterials

Typical $AgGaS_2$ nanoflowers were successfully synthesized through a simple solvothermal process with oleylamine (OA) as capping agent in the mixed solvents of 1-octyl alcohol (octanol) and cyclohexane. Fig. 1a shows that uniform flower-like nanostructures are the exclusive products when the reaction was carried out at 180 °C for 12 h, which means $AgGaS_2$ nanoflowers can be produced in large scale by this method. The average size of the as-prepared flower-like products is about 50 nm in diameter. The rough surface and evident boundaries shown in the magnified TEM image (Fig. 1b) imply that the 3D flower-like nanostructures are built by primary nanocrystals with the size about 5 nm in dimension. The size of the obtained $AgGaS_2$ nanocrystal sample calculated by Scherrer equation ($D=K\lambda/\beta\cos\theta$; $K=0.89$, $\lambda=0.154$ nm, β=FWHM, θ=diffraction angle) from XRD pattern (Fig. 1c). Fig. 1c clearly indicates that all diffraction peaks of the obtained product match well with the tetragonal phase structure of $AgGaS_2$ with the *I*-42*d* space group and a tetragonal unit cell lattice parameters of $a=5.76$ Å and $c=10.3$ Å (JCPDS 73-1233). The strong diffraction peak of (1 1 2) planes implies that the normal growth of $AgGaS_2$ along 〈1 1 2〉 direction. No other impurities, such as Ag_2S, Ga_2S_3, oxides or other organic compounds, can be detected, indicating the pure phase of the obtained products. EDS analysis result further verifies the atom content ratio of Ag, Ga and S in the obtained product is 1:0.94:2.03, which agrees well with the defect structure of $AgGaS_2$ (namely, the donor defect Ag_i and acceptor defect V_{Ga}) (Fig. 1d).

3.2. HRTEM analysis and structural simulations of $AgGaS_2$ nanoflowers

The structure of $AgGaS_2$ nanoflowers was further investigated by high-resolution transmission electron microscopy (HRTEM). Fig. 2a shows that the obtained nanoflowers are not in perfect single crystal structure, but built by primary spherical nanoparticles. Close observation indicates that the 3.19 Å lattice space is consistent with the [1 1 2] *d* spacing of tetragonal $AgGaS_2$, indicating the original colloids are in crystalline structure and

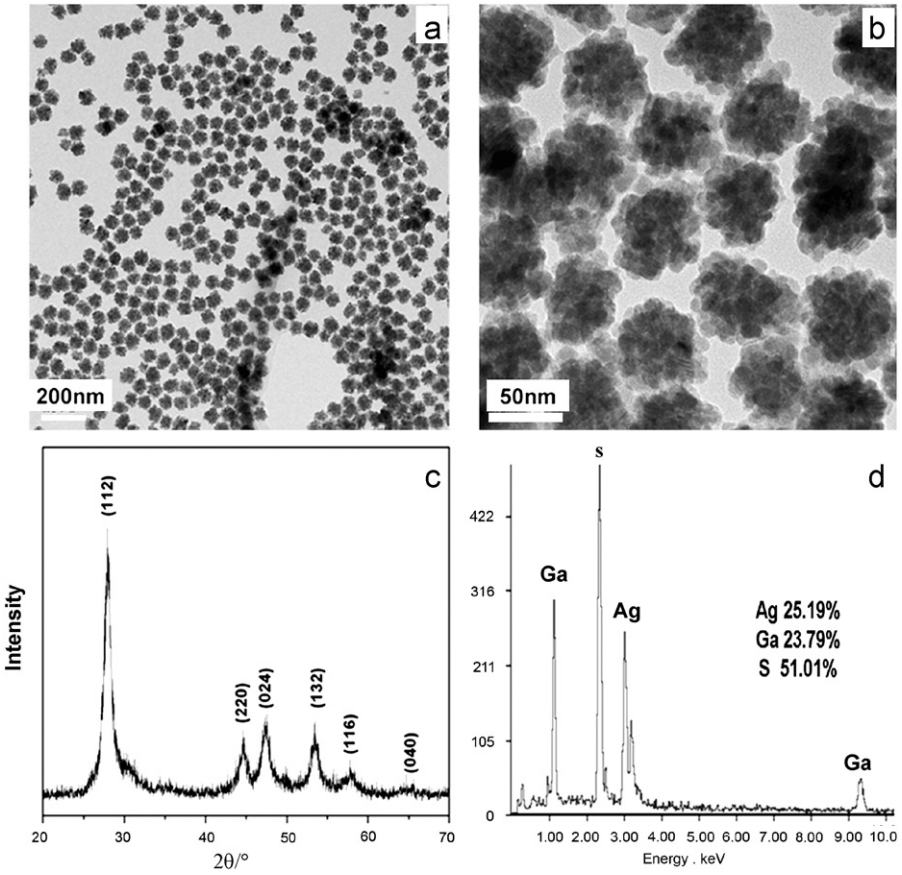

Fig. 1. TEM images (a and b), XRD pattern (c), and EDS spectrum (d) of typical $AgGaS_2$ nanoflowers prepared at 180 °C for 12 h with oleylamine (OA) as capping agent in the 1:1 mixed solvent of octanol and cyclohexane.

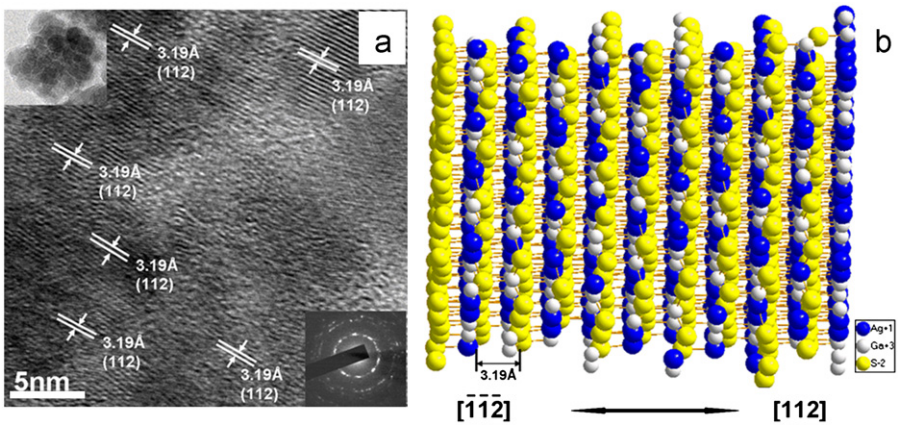

Fig. 2. HRTEM images of $AgGaS_2$ (a) and the structure side elevation images $AgGaS_2$ along ⟨1 1 2⟩ direction (b). The special coordinates of different atoms in $AgGaS_2$ are Ag (0 0 0), Ga (0 0 0 5) and S (0.29083 0.25000 0.12500).

they prefer to grow along ⟨1 1 2⟩ direction. The parallel crystallographic orientation between primary particles nearby also gives the direct evidence that the obtained flower-like nanostructures are constructed by primary colloids through oriented attachment process. According to Gibbs–Curie-Wuff's theorem, bigger crystal surface index is the general higher surface tension face, and a sequence $\gamma\{0\,0\,1\} < \gamma\{1\,0\,0\} = \gamma\{0\,1\,0\} \ll \gamma\{1\,1\,2\}$ can be deduced for tetragonal $AgGaS_2$ crystals (see Fig. 2b). Thus, $AgGaS_2$ seeds would prefer to grow along ⟨1 1 2⟩ direction because high surface energy might lead to its faster crystal facet growth, and further usually lead to the eventual disappearance of {1 1 2} facets in the final products [27]. However, the {1 1 2} facets are still maintained in the as-prepared $AgGaS_2$ colloids because of the effect of alcohol with long carbon chain and the capped effects of oleylamine (OA) in present system, which would further result in the oriented attachment of primary colloids.

3.3. *Influences of different reaction parameters on $AgGaS_2$ nanomaterials*

3.3.1. *Effects of the volume ratio of mixed solvents*

In order to synthesize $AgGaS_2$, three elements must be incorporated. Therefore, the reaction activity of the raw materials related to them should be carefully considered because separated nuclei would be generated and grown into heterostructures or even two compounds if the reaction activities of two metal precursors differ much from each other. For example, only Ag_2S and In_2S_3 rather than ternary compound could be obtained when preparing $AgInS_2$ in aqueous solution because of the different reaction rate of these binary compounds, originating from the large different value of *K*sp between Ag_2S and In_2S_3 (such as $Ksp_{Ag2S}=10^{-49.2}$, $Ksp_{In2S3}=10^{-73.2}$ in water [28]). In addition, recent researches indicated that surfactants do play an important role on the formation of inorganic compounds because the addition of complexing surfactants can affect the concentration of free ions and further affect the reaction rate and/or activity of reaction system. On the other hand, the physical or chemical properties of solvents (especially with functional groups), such as, polarity, viscosity, dielectric constant etc., also play key roles in the formation of final products, and even on the phase and shape. For instance, silver colloids with different morphologies and charming colors were obtained using pyridine, ethanol, and DMF as solvent, respectively [29]. Thus, it is reasonable to believe that suitable reaction solution will be beneficial to forming ternary chalcogenides and tuning their morphology [15,16].

In present work, a mixed solvent (cyclohexane and octanol) was designed to tune the reactivity of inorganic precursors because of their comparability. Controlled experiments reveal that the mixed solvent is beneficial for the formation of $AgGaS_2$ nanomaterials, and the morphologies or architectures of the obtained products can be easily tuned by adjusting the volume ratio of octanol to cyclohexane (Fig. 3). When the volume ratio of octanol to cyclohexane is 1:10, primary $AgGaS_2$ nanoparticles with less than 5 nm in diameter (Fig. 3a) are obtained. With the volume ratio of octanol to cyclohexane increasing to 1:5, nanoparticles with about 5 nm in size have a tendency to aggregate into the nanoflowers. When the volume ratio of octanol to cyclohexane is up to 1:1, nearly monodispersed nanoflowers with about 50 nm in diameter, built by primary nanoparticles, are fabricated. However, with the volume ratio of octanol to cyclohexane further increasing, nanoflowers are gradually dispersed into colloids, and nearly monodispersed colloids are obtained when the ratio of octanol to cyclohexane is up to 10:1. From Fig. 3f, one can see that the intensity of XRD increases with the increase of octanol concentration. The size of the $AgGaS_2$ nanocrystals formed in different octanol concentration was also calculated by the Scherrer equation, and it transformed from 4.1 nm (octanol to cyclohexane: 1:10) to ~9.0 nm (octanol to cyclohexane: 10:1).

It is well known that cyclohexane is a kind of non-polar and noncoordinating solvent with low boiling point. Therefore, the addition of cyclohexane into octanol can tune the polarity of the mixed solvent, boiling point and further affect the nucleation and the subsequent crystal growth, which would further lead to $AgGaS_2$ colloids with small size. However, these obtained nanoparticles tend to aggregate because of their high surface energy. On the other hand, octanol is a kind of poor polar solvent with long carbon chain which could increase the solubility of precursors and stabilize the formed nanocrystals [30]. It can be seen from Fig. 3d that the aggregation degree of the obtained nanoparticles reduces while the particle size of the primary building units increases slightly with the amount of octanol increasing. Finally, nearly monodispersed $AgGaS_2$ colloids are obtained on a large scale when the volume ratio of octanol and cyclohexane is up to 10:1. Further experiments reveal that the size of the obtained colloids has no obvious change even though the reaction is carried out at different reaction time and temperature. The above results demonstrate octanol not only acts as solvent but also acts as capping reagent and/or assistant surfactant (with the terminal hydroxyl of octanol) to absorb on the surface of $AgGaS_2$ colloids. Thus, nanoflowers constructed by primary nanoparticles are formed because of the incomplete protection for $AgGaS_2$ colloids when lower concentration of octanol is in the mixed solution. Nearly monodispersed $AgGaS_2$ colloids are obtained

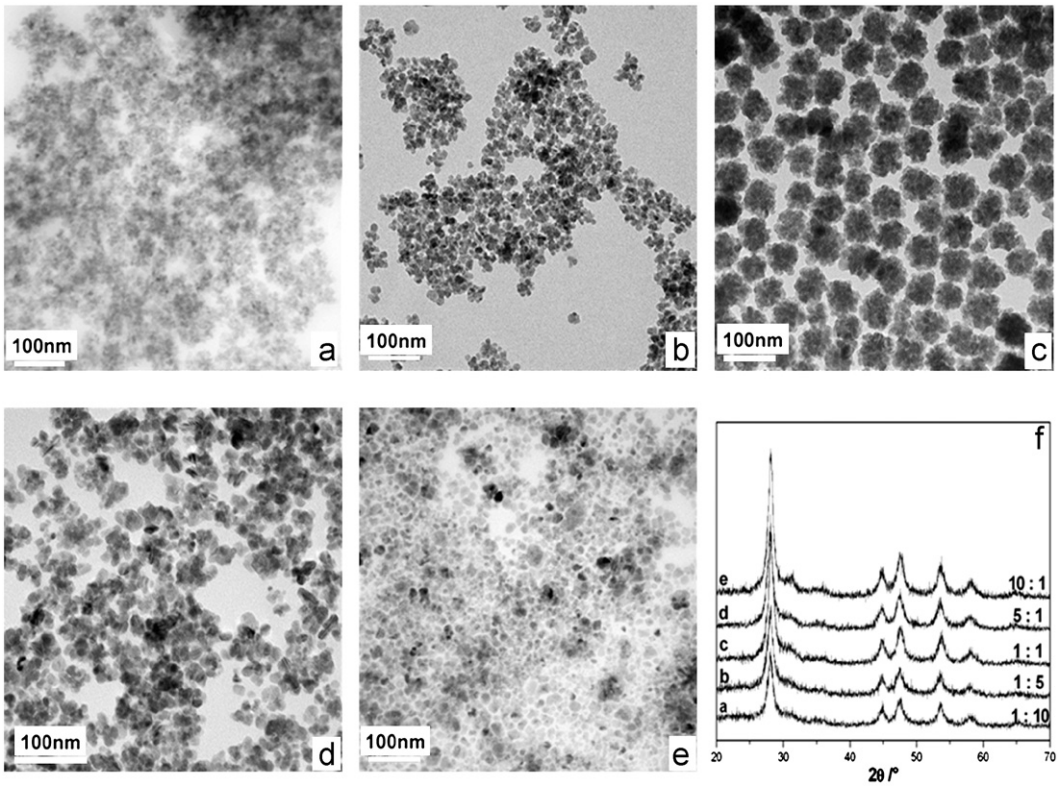

Fig. 3. (a–e) TEM images of $AgGaS_2$ synthesized in mixed solution of octanol and cyclohexane with different ratio (a) 1:10; (b) 1:5; (c) 1:1; (d) 5:1; (e) 10:1; and (f) XRD patterns of the products synthesized in different ratio of octanol to cyclohexane.

with high concentration of octanol, in which the obtained colloids are capped and protected well. Generally speaking, nanoflowers are a thermodynamically unstable species. If there were sufficient ligands and low total surface free energy in the system, nanoflowers would transform into dot-shaped nanocrystals. When the monomers were reasonably stable in solution, the nanocrystals would ripen easily which was similar to the case of In_2O_3 nanocrystals system studied by Narayanaswamy's group [31]. This was also responsible for the larger $AgGaS_2$ nanocrystals when the ratio of octanol increasing due to the increasing coordination power of long chain aliphatic alcohols [32], which was also demonstrated by the experiments below.

3.3.2. *Effects of alcohol with different carbon chain length*

The above results demonstrate that octanol plays a dual role on the synthesis of $AgGaS_2$ nanocrystals: i.e., solvent and capping reagent because of their hydrophobic chains and hydrophilic hydroxy. In order to further investigate the effects of alcohol on final products, different alcohols with various carbon chain length were introduced into the reaction system. The corresponding experiments were fulfilled in the mixed solution of different alcohol (propanol, pentanol, octanol, dodecanol, and oleyl alcohol) with cyclohexane (vol: 1:1). It can be seen from Fig. 4 that $AgGaS_2$ nanomaterials could be obtained in these mixed solutions except that their morphology has some changes. For example, diverse nanoflower-like $AgGaS_2$ particles are obtained in the mixed solution of propanol and cyclohexane (Fig. 4a). However, more uniform $AgGaS_2$ nanoflowers are obtained with the increase of carbon chain length of alcohol from propanol, pentanol to octanol. Finally, nearly monodispersed $AgGaS_2$ colloids are obtained when oleyl alcohol is added into the reaction system (Fig. 4d).

Viewed from the crystal structure of $AgGaS_2$ ("Ball and Sticks" package in Fig. 2b), one can also see that {1 1 2} facets in $AgGaS_2$ are terminated by metal ions (Ag^+ and Ga^{3+}), similar to that of tetragonal crystals $CuInS_2$ [18]. Hence, longer chain alcohol with $-OH$ would preferentially absorb on the positive polar surface of {1 1 2} which would prevent the aggregation of nanocrystals, and influence the growth of $AgGaS_2$ monomers. Furthermore, the length of carbon chain of alcohol might play an important role on their polarity or viscosity and further affects the reaction rate, the nuclei process and the following crystal growth. Therefore, insufficient surface protection because of low concentration of alcohol or shorter length carbon chain of alcohol would lead to flower-like assembled structure, and the sufficient protection would lead to the formation of nearly monodispersed colloids. To supporting this conclusion, different amount of OA was also added into the reaction system, and the relative morphology evolution of $AgGaS_2$ was provided in the Section 3.3.3.

3.3.3. *Effects of oleylamine*

As well known, organic-ligand molecules (e.g., alkyl amines, fatty acids, alkyl thiols, alkyl phosphine oxides, or some nitrogen-containing aromatics) are often used as organic solvents or capping reagents in various processes to prepare monodispersed colloids, including organic solution-phase pyrolysis, LSS (liquid–solid-solution) process, microwave-assisted methodology, solvent-less decomposition of metal thiolate single source precursors, etc. These organic-ligand molecules contain both metal coordinating groups and solvophilic groups, which could dynamically solvate nanocrystals and further control the size and/or morphology of the final products.

Fig. 5 shows the morphological change of the obtained $AgGaS_2$ with the variety of OA to AgAc. It can be found that the size of the

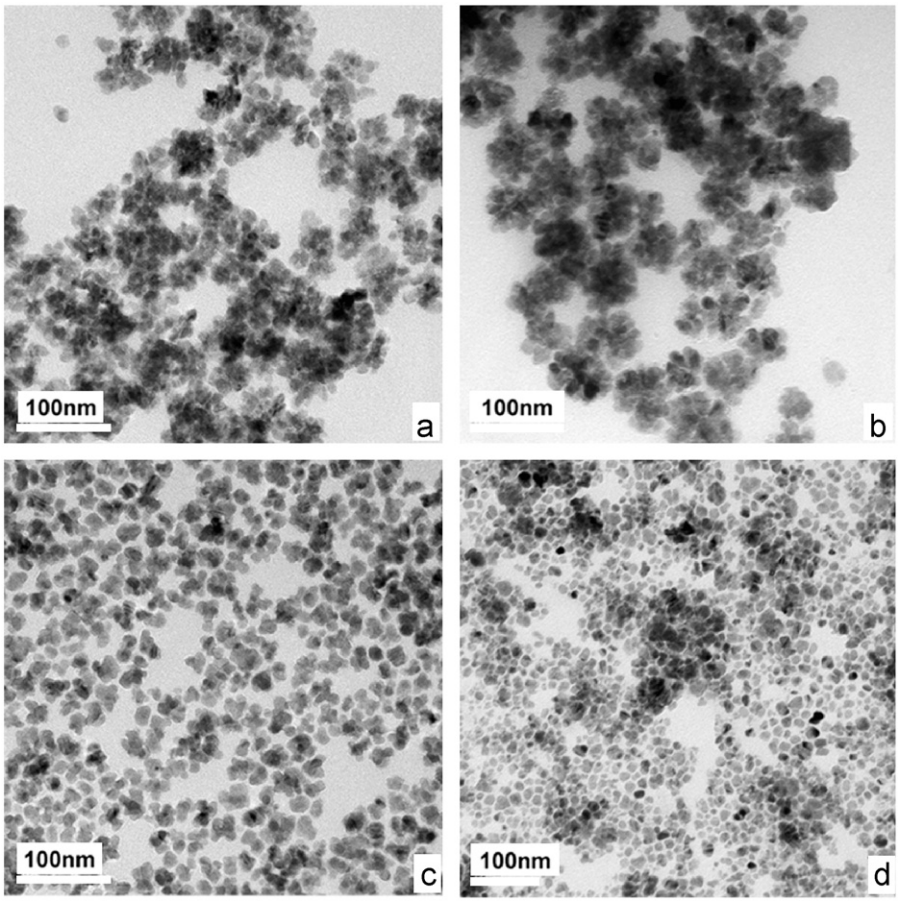

Fig. 4. (a–d) TEM images of $AgGaS_2$ synthesized in different chain lengths of alcohol with cyclohexane (vol: 1:1). (a) PPA; (b) PTA; (c) DDA; and (d) OEA.

$AgGaS_2$ flowers becomes smaller with increasing the ratio of OA to AgAc from 3:1 to 6:1. When the molar ratio of OA to AgAc exceeded that of the typical experiment, flower-like $AgGaS_2$ particles gradually transformed into dispersed nanoparticles. At last, monodispersed colloids were obtained when the molar ratio of OA to AgAc is 15:1. These results show that OA has important impact on the shape of $AgGaS_2$ nanomaterials. In present work, the newly formed H_2S from the reaction of CS_2 and water would combine with $C_{18}H_{35}NH_2$ and then yield S^{2-} and $C_{18}H_{35}NH_3^+$ in the present synthetic system. Thus, the newly formed $C_{18}H_{35}NH_3^+$ would also preferentially absorb on the negative polar surface of $\{-1\ -1\ -2\}$ facets by Coulomb's interaction, which would decrease the high surface energy of {1 1 2} and lead to the obtained products in nanoflower shape or monodispersed morphology [18]. In other words, monodispersed $AgGaS_2$ colloids or nanoflowers can be prepared by virtue of the sufficient or insufficient protection of OA. Besides, it is found in our synthesized process that OA is not only beneficial for the dissolution of AgAc precursor, but also very important for the formation of $AgGaS_2$ because it may provide necessary alkaline environment. Only black Ag_2S was obtained without OA.

3.3.4. *Effects of reaction time and temperature*

In order to further investigate the morphology evolution of $AgGaS_2$ nanoflowers, controlled experiments with different reaction time were carried out and the corresponding results are shown in Fig. 6. Results indicate that $AgGaS_2$ nanocrystals tended to aggregation and growth into nanoflower-like particles once nuclei formed, and some of irregular nanoflower-like particles are formed with 2 h (Fig. 6a). With the reaction time increasing from 6 to 24 h, the obtained $AgGaS_2$ nanoflower-like particles gradually enlarge and become uniform (Fig. 6b–d). Along with reaction time extending to 48 or 72 h, the primary $AgGaS_2$ built blocks will be fused (Fig. 6e and f).

In this synthetic system, long chain aliphatic alcohols also can play a role of stabilizing agent for growing nanocrystals [30]. With the reaction time increasing, the reaction system tends to solubility/stability and can be coupled with larger nanocrystals at the expense of smaller ones by Ostwald ripening [33,34]. This morphological evolution of $AgGaS_2$ nanoflower-like particles might be due to the following reasons: the increasing size of building blocks along with the reaction time would be beneficial for the dispersion of nanoflower-like particles by the effect of OA and long chain aliphatic alcohols. On the other hand, more organic ligand molecules might further preferentially cap on the surface of the yielded nanocrystals during the growth and ripening process, which would result in sufficient protection and monodispersed colloids.

Further experiments also reveal that tetragonal $AgGaS_2$ can be prepared in a wider temperature range (120–200 °C). From the TEM images of $AgGaS_2$ colloids synthesized at different reaction temperature for 12 h (Fig. 7), it is found that the morphologies of $AgGaS_2$ colloids varied greatly with reaction temperature. Too lower or higher reaction temperature is not beneficial for the formation of monodispersed nanoflowers, and 180 °C is the most suitable reaction temperature for $AgGaS_2$ colloids (Fig. 1a and b).

3.4. *Optical properties of $AgGaS_2$ nanomaterials*

The UV–vis absorption spectra (Fig. 8, left) reveal that no obvious difference can be observed for $AgGaS_2$ nanoflowers and

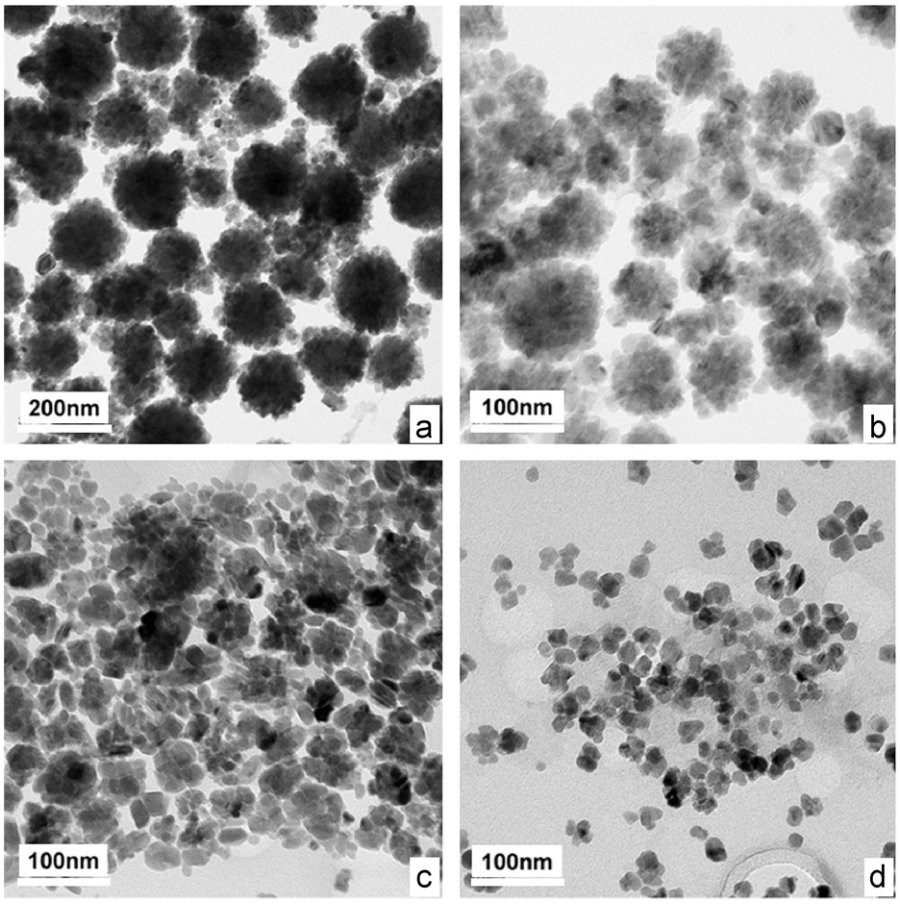

Fig. 5. (a–d) TEM images of $AgGaS_2$ synthesized with different ratio of OA to AgAc. (a) 3:1; (b) 6:1; (c) 12:1; and (d) 15:1.

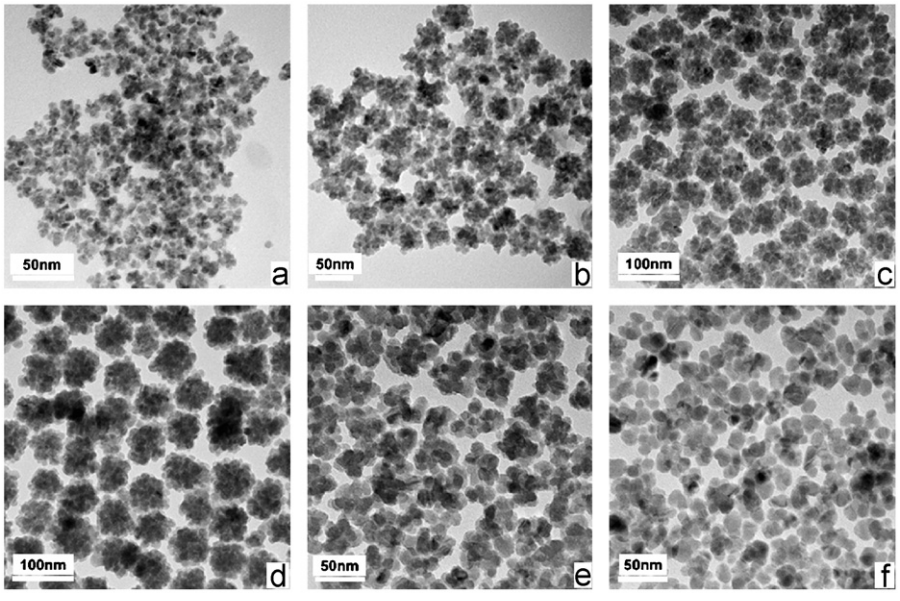

Fig. 6. (a–d) TEM images of $AgGaS_2$ synthesized in the mixture of octanol and cyclohexane (vol: 1:1) for different reaction time: (a) 2 h; (b) 6 h; (c) 12 h; (d) 24 h; (e) 48 h; and (f) 72 h.

colloids, and both of them have absorption below 480 nm, implying their similar structure. From room temperature photoluminescence spectra (Fig. 8, right), one can see that $AgGaS_2$ nanoflowers and colloids have an emission peak at 476 and 488 nm, respectively, when they are excited by 410 nm wavelength light. And both of them are blue-shift compared to that of bulk $AgGaS_2$ near 500 nm, implying the quantum size effect of the obtained $AgGaS_2$. Furthermore, the emission peak of $AgGaS_2$ colloids is red shift with 12 nm than that of nanoflower-like particles, also implying its size is slightly larger than that of the primary nanoparticles of nanoflowers. The PL band of $AgGaS_2$ could be attributed to donor–acceptor pair's recombination (DAP) [35].

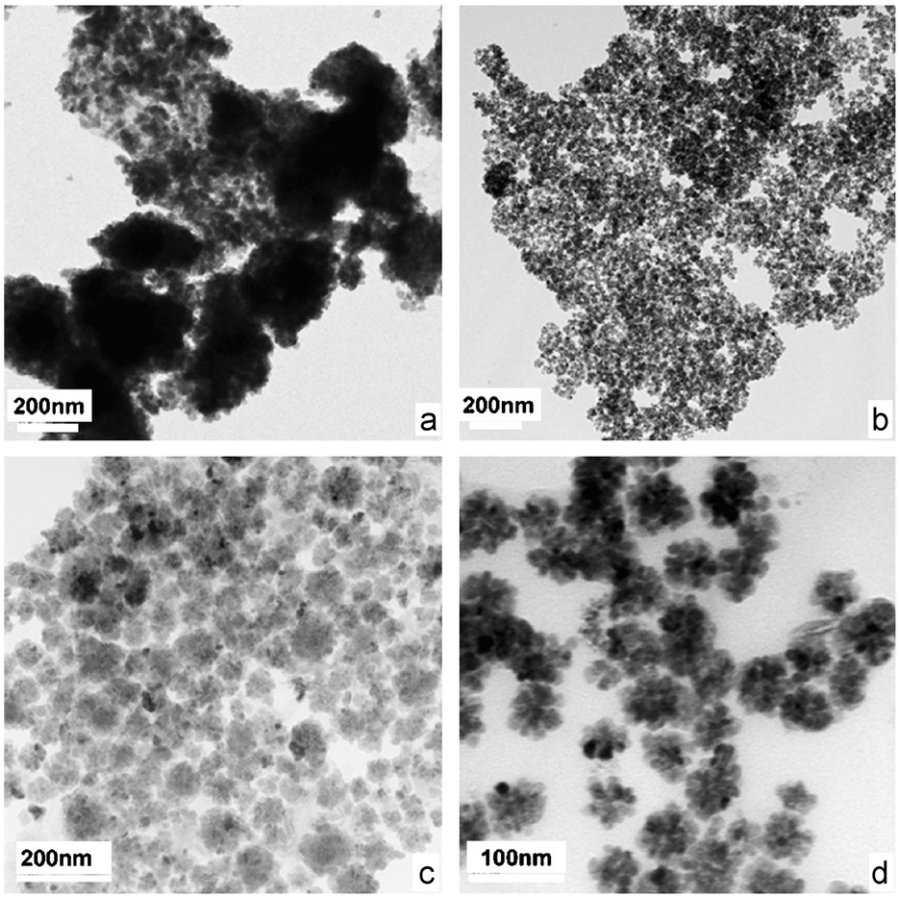

Fig. 7. TEM images of $AgGaS_2$ synthesized at different reaction temperature for 12 h: (a) 120 °C; (b) 140 °C; (c) 160 °C; and (d) 200 °C.

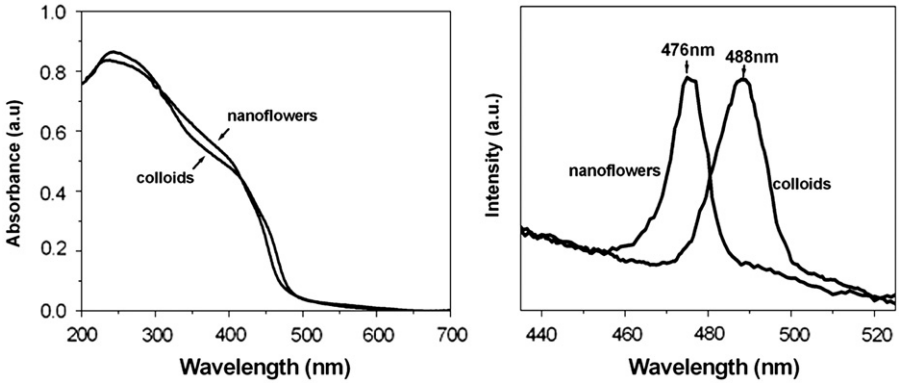

Fig. 8. UV–vis absorption spectra (left) and room temperature photoluminescence spectra (right) of $AgGaS_2$ nanoflowers (Sample 1) and colloids (Sample 5).

According to Hawn-Choi et al.'s work [36], the energy of photons emitted by DAP recombinations is given in first approximation by the equation:

$$E(r) = E_g - (E_a + E_d) + \frac{e^2}{\varepsilon r}$$

where E_g is the band gap energy; E_a and E_d are the ionization energies of acceptors and donors; and ε is the dielectric constant of the lattice. Pairs located in adjacent lattice sites present the strongest coulomb interaction and their recombination will result in emission of photons with larger energy. The $AgGaS_2$ PL properties varied with difference morphology may be beneficial for its different device applications.

3.5. Surface photovoltage (SPV) properties of $AgGaS_2$

The SPV effect, produced by a change of the surface potential caused by illumination, has been successfully applied to investigate electron process in semiconductors, and it is considered as a simple and precise method for understanding interfacial electron transfer in semiconductors [37,38]. Fig. 9 shows the surface photovoltage spectra (SPS) of $AgGaS_2$ nanoflower-like particles. From the curve of 0 V, it is found that the photovoltage response of $AgGaS_2$ nanoflower powders appears from 330 to 580 nm, which is consistent with the solid diffuse reflection. This result implies that $AgGaS_2$ can absorb photons and separate electron–hole pairs in the built-in electric field. Furthermore,

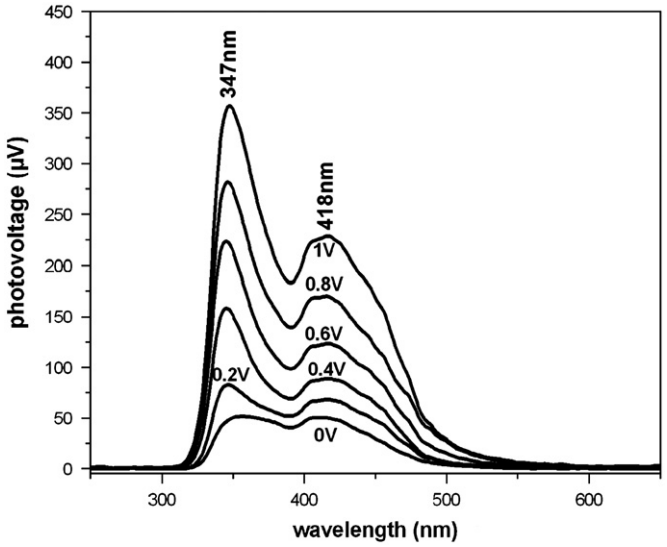

Fig. 9. Surface photovoltage spectra of $AgGaS_2$ nanoflower-like particles under the biases from 0 to 1 V.

the photovoltage response becomes stronger when an extra electric field (EEF) is applied, and the change of the 347 nm peak is more distinct than that of 418 nm peak by the enhancement of EEF. The above phenomena could be explained by the surface photovoltage mechanism and the structure of $AgGaS_2$ nanomaterial. In SPS experiments, the SPV is monitored as a function of photo energy, and the formation of SPV requires both photogeneration and separation of charge carries. The former requires semiconductors with a suitable band gap, while the latter requires the efficient separation and transportation of electron–hole pairs under a built-in electric field. Thus $AgGaS_2$ nanomaterials provided a chance for photogeneration and efficient separation of charge carrier, a suitable EEF could not only function as a built-in field, but also servers as the carriers go beyond the potential barriers, and an enhancement photovoltage response appeared under EEF, which may be beneficial for manipulation on various optical applications of $AgGaS_2$ nanomaterials.

4. Conclusions

A mixed solvent synthetic system was elaborately designed to prepare ternary chalcogenide $AgGaS_2$, and monodispersed $AgGaS_2$ nanoparticles with controlled shape and size were obtained with simple inorganic salts as precursors. Further studies revealed that the morphology of the obtained $AgGaS_2$ had undergone a transformation from nanoflowers to colloids by adjusting the ratio of cyclohexane and 1-octyl alcohol or the carbon chain length of alcohol and/or the molar ratio of OA. This simple mixed solvent–thermal system made it possible to have a systematic study of the reaction mechanism along with the growth kinetics of nanocrystals. Furthermore, the PL and SPV research should be valuable for further theoretical and practical of optical activity of $AgGaS_2$ nanomaterials.

Acknowledgment

The work was supported by National Natural Science Foundation of China (21071097), National Basic Research Program of China (2009CB930400), and the key project of State Key Laboratory of High Performance Ceramics and Superfine Microstructure (SKL200901SIC).

References

[1] I. Gur, N.A. Fromer, M.L. Geier, A.P. Alivisatos, Science 310 (2005) 462–465.
[2] M.G. Panthani, V. Akhavan, B. Goodfellow, J.P. Schmidtke, L. Dunn, A. Dodabalapur, P.F. Barbabra, B.A. Korgel, J. Am. Chem. Soc. 130 (2008) 16770–16777.
[3] D. Li, J.T. McCann, Y.N. Xia, Small 1 (2005) 83–86.
[4] W.U. Huynh, J.J. Dittmer, A.P. Alivisators, Science 295 (2002) 2425–2427.
[5] Y.N. Xia, P.D. Yang, Y.G. Sun, Y.Y. Wu, B. Mayers, B. Gates, Y.D. Yin, F. Kim, H.Q. Yan, Adv. Mater. 15 (2003) 353–389.
[6] Y.D. Yin, A.P. Alivisatos, Nature 437 (2005) 664–670.
[7] A.Z. Peng, X.G. Peng, J. Am. Chem. Soc. 124 (2002) 3343–3353.
[8] K. Yoshino, T. Ikari, S. Shirakata, H. Miyake, K. Hiramatsu, Appl. Phys. Lett. 78 (2001) 742–744.
[9] S.C. Eewin, I. Zutic, Nat. Mater. 3 (2004) 410–414.
[10] M. Nanu, J. Schoonman, A. Goossens, Nano Lett. 5 (2005) 1716–1719.
[11] H.L. Peng, D.T. Schoen, S. Meister, X.F. Zhang, Y. Cui, J. Am. Chem. Soc. 129 (2007) 34–35.
[12] D.C. Pan, L.J. An, Z.M. Sun, W. Hou, Y. Yang, Z.Z. Yang, Y.F. Lu, J. Am. Chem. Soc. 130 (2008) 5620–5621.
[13] H.Z. Zhong, Y. Zhou, M.F. Ye, Y.J. He, J.P. Ye, C. He, C.H. Yang, Y.F. Li, Chem. Mater. 20 (2008) 6434–6443.
[14] L. Tian, H.I. Elim, W. Ji, J.J. Vittal, Chem. Commun. (2006) 4276–4278.
[15] D.S. Wang, W. Zheng, C.H. Hao, Q. Peng, Y.D. Li, Chem. Commun. (2008) 2556–2558.
[16] X.L. Gou, F.Y. Cheng, Y.H. Shi, L. Zhang, S.J. Peng, J. Chen, P.W. Shen, J. Am. Chem. Soc. 128 (2006) 7222–7229.
[17] B. Koo, R.N. Patel, B.A. Korgel, J. Am. Chem. Soc. 131 (2009) 3134–3135.
[18] W.M. Du, X.F. Qian, J. Yin, Q. Gong, Chem. Eur. J 13 (2007) 8840–8846.
[19] H. Matthes, R. Viehmann, N. Marschall, Appl. Phys. Lett. 26 (1975) 237–239.
[20] G.D. Boyd, H.M. Kasper, J.H. McFee, J. Appl. Phys. 44 (1973) 2809–2812.
[21] V.G. Dmitriev, G.G. Gurzadyan, D.N. Kosasyon, Handbook of Nonlinear Optical Crystals, in: A.E. Siegman (Ed.), Springer Series in Optical Science, vol. 64, Springer Verlag, 1991, pp. 82–83 158–159, 173–179, 189–191.
[22] L.D. Gulay, O.V. Parasyuk, J. Alloys Comp. 327 (2001) 100–103.
[23] M. Kurasawa, S. Kobayashi, F. Kaneko, K. Oishi, S.I. Ohta, J. Cryst. Growth 167 (1996) 151–156.
[24] J.Q. Hu, B. Deng, K.B. Tang, Q.Y. Lu, R.R. Jiang, Y.T. Qian, Solid State Sci. 3 (2001) 275–278.
[25] J.Q. Hu, Q.Y. Lu, K.B. Tang, Y.T. Qian, G.E. Zhou, X.M. Liu, Chem. Commun. (1999) 1093–1094.
[26] D.C. Pan, X.L. Wang, H. Zhou, C.L. Xu, Y.F. Lu, Chem. Mater. 21 (2009) 2489–2493.
[27] G. Wulff, Z. Krystallogr. 34 (1901) 449–530.
[28] J.A. Dean (Eds), Lange's Handbook of Chemistry, fifteenth ed. 8.10, 8.15.
[29] R. He, X.F. Qian, J. Yin, Z.K. Zhu, J. Mater. Chem. 12 (2002) 3783–3786.
[30] D. Caruntu, K. Yao, Z.X. Zhang, T. Austin, W.L. Zhou, C.J. O'Connor, J. Phys. Chem. C. 114 (2010) 4875–4886.
[31] A. Narayanaswamy, H.F. Xu, N. Pradhan, M.S. Kim, X.G. Peng, J. Am. Chem. Soc. 128 (2006) 10130–103019.
[32] Z. Cheng, L. Huang, J. He, Y. Zhu, S. O'Brien, J. Mater. Res. 21 (2006) 3187–3195.
[33] M.S. Mo, S.H. Lim, Y.W. Mai, R.K. Zheng, S.P. Ringer, Adv. Mater. 20 (2008) 339–342.
[34] Y.F. Chen, M. Kim, G.D. Lian, M.B. Johnson, X.G. Peng, J. Am. Chem. Soc. 127 (2005) 13331–13337.
[35] M. Marceddu, A. Anedda, C.M. Carbonaro, D. Chiriu, R. Corpino, P.C. Ricci, Appl. Surf. Sci. 253 (2006) 300–305.
[36] Hawn-In Choi, Sung-Hawn Eom, P.Y. Yu, Phys. Status Solidi B. 215 (1999) 99–104.
[37] L. Frank, K. Jessica, B. Shelly, B. Keith, G. Michael, G. Doron, R. Sven, C. David, J. Phys. Chem. B. 105 (2001) 6347–6352.
[38] X. Wei, T.F. Xie, D. Xu, Q. Zhao, S. Pang, D.J. Wang, Nanotechnology 19 (2008) 275707.